Electronic and Structural Shell Closure in AgCu and AuCu Nanoclusters

Giovanni Barcaro,[†] Alessandro Fortunelli,*[,†] Giulia Rossi,[‡] Florin Nita,[‡,§] and Riccardo Ferrando*[,‡]

IPCF/CNR, Via G. Moruzzi 1, Pisa, I56124, Italy, Dipartimento di Fisica, Università di Genova, INFM and IMEM/CNR, Via Dodecaneso 33, Genova, I16146, Italy, and Institute of Physical Chemistry IG Murgulescu, Romanian Academy, Spl. Independentei 202, Bucharest, Romania

Received: July 20, 2006; In Final Form: September 19, 2006

The structures of AgCu clusters containing 40 atoms are investigated. The most promising structural families (fcc clusters, capped decahedra, and two types of capped polyicosahedra) are singled out by means of global optimization techniques within an atom−atom potential model. Then, representative clusters of each family are relaxed by means of density-functional methods. It is shown that, for a large majority of compositions, a complex interplay of geometric and electronic shell-closure effects stabilizes a specific polyicosahedral family, whose clusters are much lower in energy and present large HOMO−LUMO gaps. Within this family, geometric and quantum effects concur to favor magic structures associated with core−shell chemical ordering and high symmetry, so that these clusters are very promising from the point of view of their optical properties. Our results also suggest a natural growth pathway of AgCu clusters through high-stability polyicosahedral structures. Results for AuCu clusters of the same size are reported for comparison, showing that the interplay of the different effects is highly material specific.

1. Introduction

Metallic nanoclusters, namely aggregates of metal atoms of nanometric size, present physical and chemical properties which can be strongly size-dependent,[1−4] thus offering the possibility of tuning specific properties by selecting the cluster size. These size-dependent properties are interesting not only from the point of view of basic science but also for applications in nanotechnology and heterogeneous catalysis.

In this context, nanoscale clusters of coinage metals have been widely studied from both the experimental and theoretical point of view.[5−7] Their interaction with oxygen, carbon monoxide, methanol, and nitrogen in the gas phase has been intensively studied in view of understanding their role as catalysts in specific chemical reactions, such as CO and hydrocarbon oxidation.[8−12] They are also of great practical importance because of their peculiar optical properties,[13−15] especially when core−shell arrangements are achieved.

Recently, binary coinage metal clusters have attracted considerable attention.[16−22] In fact, binary clusters offer an extra degree of freedom for catalysis and nanotechnology applications, since in these clusters one can vary both size and composition.[23] The starting point for determining, and possibly tuning, the properties of a binary cluster of given size and composition is the knowledge of its structure. Pure clusters may present a large variety of possible structures, including high-symmetry structural motifs such as fcc-truncated octahedra, icosahedra, and decahedra.[4] Binary clusters offer an even wider spectrum of possible structural motifs, and within each motif, different kinds of chemical ordering are possible: intermixed, core−shell, and multishell.[24−26]

For these reasons, the determination of the best structures of binary clusters is a very challenging task. As a starting point, indications on the possible structures may come from geometric and electronic shell closure considerations, corresponding to geometric and electronic magic numbers. In the case of pure coinage metals, the photoelectron spectra of clusters containing a few tens of atoms have revealed electronic shell structures with clear closures corresponding to those of spherical electron gas models.[27−32] These results indicate that coinage metals behave, at least approximately, as simple metals, with each atom contributing a single quasi-free electron. The electronic shell closure has also been confirmed for Ag clusters doped by a single Cu impurity,[21] with the further indication that the inclusion of the impurity somewhat enhances the shell closure effect. However, these considerations are not sufficient for determining the actual structure of the clusters.

In this paper we analyze binary AgCu clusters of size $N = 40$ atoms at varying composition and compare the results to those for AuCu clusters of the same size. This size is especially important for two reasons. First of all, it is a magic electronic size for both the hard-wall and the harmonic jellium (spherical electron gas) model[33] and the Tensor Surface Harmonic Theory[34,35] (as modified to describe nonhollow clusters[36]); hence we expect quantum effects, possibly connected with spherical aromaticity,[37,38] to play a significant role. Second, at $N = 40$, there is a competition among several structural motifs, from bulklike fcc clusters, to capped decahedra, to two distinct families of polyicosahedra. Sizes $N = 34$ and $N = 38$, which were studied previously,[17−19,39] lack some of these features. Size 34 is magic for the hard-wall but not for the harmonic electron gas model. Moreover, at size 34, there is practically no competition among motifs, since there is a clearly dominant specific polyicosahedral family. Size 38 presents a competition among several motifs, but it is not an electronic magic size.

* Corresponding author: A.F., fortunelli@ipcf.cnr.it; R.F., ferrando@fisica.unige.it.
[†] IPCF/CNR.
[‡] Dipartimento di Fisica, Università di Genova, INFM and IMEM/CNR.
[§] Institute of Physical Chemistry IG Murgulescu, Romanian Academy.

10.1021/jp064593x CCC: $33.50
Published on Web 10/26/2006

In the following we show that the most stable structural motif of AgCu clusters arises from a complex interplay of different factors, including geometry, chemical ordering, and electronic shell closure. These factors concur in determining a single structural family which is magic from both the electronic and the geometric point of view and occurs at almost every possible composition, with special stability when the composition allows a high-symmetry core−shell arrangement. This structural family has polyicosahedral character,[17] compact shape, and not too strained bonds (especially at intermediate compositions) and at the same time presents quite large HOMO−LUMO gaps (of the order of 0.8 eV), indicating electronic shell closure. Other structural motifs could be in principle competitive but lack at least one of these favorable factors. The fact that geometric and quantum effects concur to favor magic structures associated with core−shell chemical ordering and high-symmetry render these clusters very appealing from the point of view of their optical properties.

Results for AuCu clusters of the same size are also reported, to highlight differences which mainly originate from the stronger tendency of Au and Cu to form heterogeneous bonds, compared to Ag and Cu, and to the shorter-range character of the atom−atom interaction for gold: these differences bring two different families of polyicosahedra in close competition.

2. Computational Method

An unbiased search of the lowest-energy structures of metallic clusters of this size can be performed on fully ab initio grounds only with an intense computational effort[40] due to the huge number of local minima on the potential energy surface.[4] The case of bimetallic clusters is even much more demanding, because of the inequivalence of homotops, namely of isomers presenting the same geometric structure but a different chemical ordering.[41] For this reason, a two-step procedure is employed. First, for each composition at size 40, global optimization is performed within a second-moment tight-binding (SMTB) atom−atom potential model[42,43] (see refs 19 and 44 for the form and parameters of the potential). Even though the parameters of the potential are fitted on bulk quantities, there are indications that the potential is reasonably accurate also in low-coordination situations, such as crystal surfaces. In fact, this potential was employed in the modeling of an Ag monolayer on Cu(111), obtaining a very good agreement with the experimental results.[45] This semiempirical potential was also able to select the most important structural motifs of AgCu clusters.[17] Representative clusters of each motif are then locally optimized by density-functional-theory (DFT) calculations.

Global optimization is performed by running three different algorithms, the basin-hopping,[46] the energy-landscape paving method (ELP),[47] and the parallel excitable walkers[48] (PEW) method. These algorithms adopt a Monte Carlo (MC) plus minimization scheme.[49] At each composition, a run of 10^6 MC steps is made for each algorithm. In these long runs, the elementary MC moves are performed by displacing each atom of the cluster within a sphere of radius 1.3 Å with uniform probability. After the MC runs, the best clusters pertaining to different structural motifs are reoptimized by running low-temperature basin-hopping simulations of 10^5 steps in which only exchange moves between Ag and Cu atoms, or moves displacing single surface atoms are performed. These further simulations are aimed at the optimization of the chemical ordering and of the surface of a given kind of structure.

Density-functional calculations are then carried out on selected configurations from each structural family with the DF

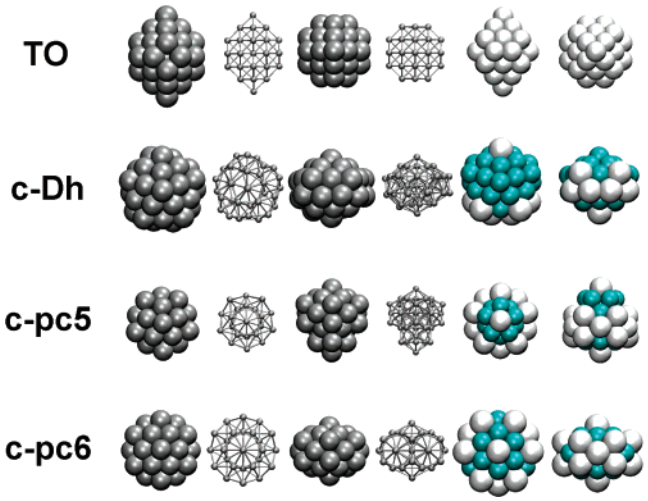

Figure 1. (First row) fcc-truncated octahedron (TO). This TO has D_{4h} symmetry. It can be obtained either by removing atoms from four vertexes over six of the complete octahedron of 44 atoms or by adding two atoms on opposite square facets of the 38-atom fully symmetric truncated octahedron. In the first four snapshots from left, the structure is shown from different viewpoints. In the fifth and sixth snapshots, the TO is shown at composition $Ag_{34}Cu_6$. Copper atoms are not visible because they form the inner core; silver atoms are in light gray. (Second row) Capped decahedron (c-Dh). This structure is obtained by adding an umbrella to the complete decahedron of 23 atoms. Depending on composition, the umbrella shape may change, but the structure is not highly symmetric, having at most a single reflection plane. In the fifth and sixth snapshots, the c-Dh is shown at composition Ag_8Cu_{32}. (Third row) Capped 5-fold pancake (c-pc5). This structure is a polyicosahedron obtained by adding an umbrella of 6 atoms on the 5-fold pancake of 34 atoms.[17] The first four snapshots show the structure from different viewpoints. In the fifth and sixth snapshots, the c-pc5 is shown at composition $Ag_{17}Cu_{23}$, where it has C_{5v} symmetry. (Fourth row) Capped 6-fold pancake (c-pc6). This structure is obtained by adding 2 vertex atoms to the 6-fold pancake,[17] a polyicosahedron of 38 atoms. In the fifth and sixth snapshots, the c-pc6 is shown at composition $Ag_{17}Cu_{23}$, where it has D_{3h} symmetry.

module of the NWChem package[50] (release 4.7) and use the Becke functional[51] for exchange and the Perdew−Wang functional[52] for correlation. Gaussian-type-orbital basis sets (7s6p6d)/[5s3p2d] and effective core potentials are used for all elements, derived from refs 53 and 54 for Ag and ref 55 for Cu, and modified combining the suggestions in refs 56 and 57. Charge density fitting (11s4p5d3f4g)/[11s4p4d3f2g] Gaussian-type-orbital basis sets were used to compute the Coulomb potential.[58] All the calculations have been performed spin-unrestricted and using a Gaussian-smearing technique[59] for the fractional occupation of the one-electron energy levels. A numerical grid of 65 radial points and 350 points for the angular part was used for evaluation of the exchange-correlation potential and energy. The geometry optimization was stopped when the numerical force on atoms was less than 4×10^{-4} au. More details on the numerical procedure can be found in ref 57.

3. Structural Motifs from Atom−Atom Potential Optimization

The global optimization runs using the Gupta-like potential have singled out four possible structural motifs (see Figure 1).

The first motif is represented by fcc clusters, namely pieces of fcc bulk crystal (Cu, Ag, and Au present the fcc lattice in their bulk form). This is the only motif which does not present any local 5-fold symmetry axis.

The clusters belonging to the second motif can be described as decahedra of 23 atoms capped by a distorted umbrella of 17

atoms. In the following, this motif will be referred to as the capped decahedral motif (c-Dh). Depending on composition, the umbrella can be of different shapes. In some cases, the umbrella is placed in such a way that this cluster is a fragment of the icosahedron of 55 atoms. Structures of this kind were found in the optimization of pure Sutton-Chen Ag_{40} and Cu_{40} clusters[60] and in the optimization of Cu_{40}, $Au_{10}Cu_{30}$, $Au_{20}Cu_{20}$ within the Gupta model.[16]

The clusters belonging to the third and fourth motifs are different families of polyicosahedra. Polyicosahedra are clusters built up by interpenetrating elementary icosahedra of 13 atoms.[17] The structures of the third motif are a 34-atom polyicosahedra (the 5-fold pancake, see Figure 1 of ref 17) capped by 6 atoms. These clusters will be referred to as capped 5-fold pancakes (c-pc5) in the following. When the cap is placed symmetrically around the 5-fold axis, these clusters can also be seen as incomplete anti-Mackay icosahedra missing 5 atoms, with a crown of atom vacancies placed symmetrically around the 5-fold axis. For some specific compositions (like $Ag_{27}Cu_{13}$, $Ag_{22}Cu_{18}$, $Ag_{17}Cu_{23}$) these clusters belong to the C_{5v} symmetry group. The clusters of the fourth motifs can be described as 6-fold pancake structures (see Figure 1 of refs 17 and 39) capped by two silver atoms along the 6-fold symmetry axis. For this reason, they will be referred to as capped 6-fold pancakes (c-pc6) in the following. For some specific compositions, these clusters can be of D_{6h} symmetry, thus being the most symmetric clusters found at size 40. A cluster of this structure was found to be the global minimum of $Au_{10}Cu_{30}$ within the Gupta model[16] and of Al_{40} using an embedded-atom potential.[61]

The results of the SMTB model indicate that, depending on composition, capped decahedra, c-pc5, and c-pc6 are the global minima. No fcc global minima are found, even though fcc clusters are in close competition with the other motifs for homogeneous clusters. Capped decahedral global minima are found for homogeneous Ag and Cu clusters,[7] for copper-rich compositions from Cu_{40} to $Ag_{11}Cu_{29}$, and for silver-rich compositions from Ag_{40} to $Ag_{37}Cu_3$. Capped 6-fold pancakes (c-pc6) are the global minima in the ranges from $Ag_{36}Cu_4$ to $Ag_{33}Cu_7$ and from $Ag_{20}Cu_{20}$ to $Ag_{12}Cu_{28}$. Finally, c-pc5 structures are the global minima in the range from $Ag_{32}Cu_8$ to $Ag_{21}Cu_{19}$. As we shall see below, the DFT local optimizations of the clusters belonging to the four families will reveal a different scenario, arising from the different electronic effects on the relative energetics of the structural motifs.

4. DFT Optimization of Homogeneous Ag and Cu Clusters

The DFT local relaxation of the structures described in the previous section shows that homogeneous Ag and Cu clusters exhibit a different energy ordering of the four motifs. For Ag, the capped Dh and the fcc cluster are almost degenerate, whereas polyicosahedra are clearly higher in energy, especially the c-pc6. For Cu, the c-pc5 is the lowest in energy, and it is appreciably separated from the capped decahedron and the fcc cluster. Even though we cannot claim that we have considered the best capped decahedron, there is a clear indication that the c-pc5 is competitive for Cu_{40}, whereas for Ag_{40} it is not. This result agrees with a qualitative trend derived from the semiempirical potential modeling. In fact, c-pc5 structures are highly strained, with strongly compressed inner atoms.[17] Compared to Ag, Cu is able to better accommodate this compression,[4] paying a smaller energy penalty, whereas for Au the energetic penalty would be larger. Inner atoms in c-pc6 structures are less compressed,[39] so the SMTB model would favor them compared to c-pc5 structures for homogeneous clusters. Surprisingly, the DFT calculations indicate the opposite. The reasons why the c-pc6 structures are destabilized with respect to c-pc5 structures are purely electronic in character and thus are not included in the SMTB approach. In fact, structures of type c-pc5 generally present an electronic shell closure effect, whereas c-pc6 structures present an electronic shell *un*closure effect.[18] Indeed, as shown in Table 1, c-pc5 structures present large HOMO−LUMO gaps, whereas c-pc6 clusters are Jahn−Teller structures with very small gaps. To further rationalize this point, we performed an extended Hückel (or tight-binding) calculation, i.e., we assigned to each atom an s-type atomic orbital, interacting with neighboring atomic orbitals through a distance-dependent Slater-like analytic form, $H_{ij} = -11.2\delta_{ij} - A \exp(-r_{ij}/r_0)$,[62] and we diagonalized the corresponding Hamiltonian matrix. This is the simplest model which can take into account quantum (shell closure/unclosure) effects. The density-of-states (DOS) typically obtained for c-pc5 and c-pc6 structures is shown in Figure 2. From an inspection of this figure, it is apparent that c-pc5 structures exhibit significant energy gaps at both 34 and 40 electrons, whereas c-pc6 structures do not. Assuming the usual ordering of electronic states in a spherical potential,[33,35,37] 1s1p1d2s1f2p1g..., with shell closures at $N = 34$ (1s1p1d2s1f) and $N = 40$ (1s1p1d2s1f2p), we see that the oblate deformation of c-pc6 structures destabilizes the 2p orbitals, bringing them to intermix with the 1g orbitals, thus destroying the shell closure at $N = 40$. We note in this connection that all the 2p orbitals are destabilized, also because their radial node is associated with antibonding interactions, more numerous in the c-pc6 structure due to the larger number of intershell contacts (this is also true for the 2s orbitals). The more oblate character of the c-pc6 structure implies a greater splitting of the 1g orbitals compared to the c-pc5 structure.

TABLE 1: Structure, Symmetry Group, Spin, HOMO−LUMO Gap, and Separation from the Lowest Minimum ΔE for Structures Pertaining to the Different Structural Motifs of Homogeneous Ag and Cu Clusters

composition	structure	group	spin	gap (eV)	ΔE (eV)
Cu_{40}	c-pc5[b]	C_{5v}	0	0.77	0.00
Cu_{40}	c-Dh[a]	C_i	1	0.25/0.17	0.36
Cu_{40}	TO[d]	C_{4v}	1	0.49/0.16	0.46
Ag_{40}	c-Dh	C_i	0	0.02	0.00
Ag_{40}	TO	D_{4h}	1	0.32/0.18	0.03
Ag_{40}	c-pc5	C_{5v}	0	0.73	0.64
Ag_{40}	c-pc6[c]	D_{6h}	0	0.05	1.19

[a]Capped decahedra. [b] Capped 5-fold pancakes. [c]Capped 6-fold pancakes. [d]fcc-truncated octahedra.

5. DFT Optimization of Binary AgCu Clusters

There are several reasons to expect that polyicosahedral structures become more favorable for binary than for homogeneous clusters. The difference in atomic radii (the atomic size mismatch, which is already effective for binary noble gas clusters[63]), bond-order/bond-length correlation of metallic bonding,[64] and the smaller surface energy of Ag with respect to Cu, producing a tendency to surface segregation of Ag, all concur to the formation of polyicosahedral core−shell clusters with considerably reduced internal tension. However, all these considerations apply to both c-pc5 and c-pc6 structures. Indeed, c-pc5 structures would be better stabilized by an even larger difference in atomic radii,[39] whereas for c-pc6 the difference in atomic radii between Ag and Cu atoms is close to optimal. We have seen that the results of the global optimization within the atom−atom SMTB potential confirm this prediction, since

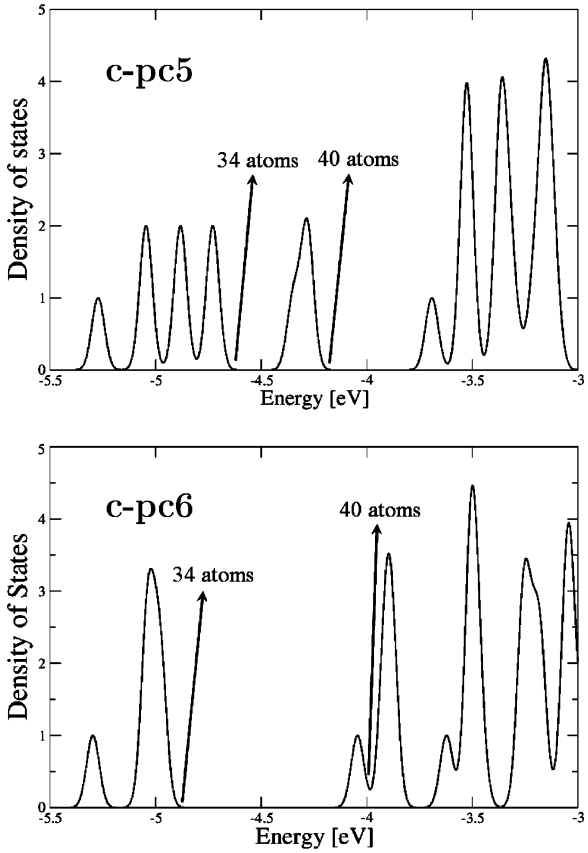

Figure 2. DOS derived from extended Hückel calculations on typical c-pc5 and c-pc6 structures. Energies in eV, DOS in arbitrary units. A broadening factor of 0.03 eV has been used to transform the delta functions into Gaussians. First 20 electrons are not shown for c-pc5; the first 22 electrons are not shown for c-pc6 (the lowest 1f orbital in c-pc6 lies at −6.3 eV). The occupations corresponding to $N = 34$ and $N = 40$ electrons are indicated by arrows. The peak of the c-pc6 DOS where the Fermi energy falls is a mixture of 2p and 1g states. The DFT DOS are qualitatively similar to those in the figure.

the majority of (putative) global minima have polyicosahedral character, and among polyicosahedral minima, there is a fair proportion of c-pc5 and c-pc6.

The DFT analysis leads to a different scenario. Polyicosahedral structures become even more dominant, and a specific polyicosahedral motif, the c-pc5 one, is clearly preferred at almost all compositions. As shown in Table 2, in fact, where the energy separation ΔE from the lowest isomer is reported, capped 5-fold pancakes are much lower in energy than the other structures. For example, for Ag_6Cu_{34}, the c-pc5 structure is separated from the c-Dh by more than 1 eV; for $Ag_{14}Cu_{26}$, ΔE is more than 1.7 eV below the c-Dh and the c-pc6, which are almost degenerate. Large ΔEs (of even more than 2 eV) are found also for several other compositions, from $Ag_{17}Cu_{23}$ to $Ag_{32}Cu_8$. For $Ag_{34}Cu_6$, ΔE is somewhat reduced, and the c-pc6 structure is separated by only 0.7 eV.

The enhanced stability of the c-pc5 structures can be explained in terms of the above-mentioned electronic shell closure effect: c-pc5 clusters present large HOMO−LUMO gaps at all compositions, even at those at which the C_{5v} symmetry cannot be attained. On the opposite, clusters pertaining to c-Dh, c-pc6, and TO motifs present small gaps, indicating electronic shell unclosure. The stability of c-pc5 clusters is thus due to the synergic effect of geometric magic arrangement and electronic shell closure. As we shall see in the following, this synergic effect is peculiar of AgCu and is not found in AuCu.

TABLE 2: Structure, Symmetry Group, Spin, HOMO−LUMO Gap, and Separation from the Lowest Minimum ΔE for Structures Pertaining to the Different Structural Motifs of Heterogeneous AgCu Clusters

composition	structure	group	spin	gap (eV)	ΔE (ev)	ΔE_{SMTB}[f]
Ag_6Cu_{34}	c-pc5	C_{5v}	0	0.74	0.00	0.00
Ag_6Cu_{34}	c-Dh[a]	C_i	0	0.06	1.11	−1.23
$Ag_{14}Cu_{26}$	c-pc5[b]	C_s	0	0.81	0.00	0.00
$Ag_{14}Cu_{26}$	c-Dh	C_s	0	0.17	1.41	−0.52
$Ag_{14}Cu_{26}$	c-pc6[c]	D_{6h}	1	0.39/0.22 JT	1.47	−0.65
$Ag_{16}Cu_{24}$	c-pc5	C_s	0	0.81	0.00	0.00
$Ag_{16}Cu_{24}$	c-pc6	D_{2h}	1	0.16/0.04	1.72	−0.49
$Ag_{16}Cu_{24}$	c-Dh	C_i	1	0.19/0.10	1.77	−0.32
$Ag_{17}Cu_{23}$	c-pc5	C_{5v}	0	0.79	0.00	0.00
$Ag_{17}Cu_{23}$	c-pc6	D_{3h}	1	0.38/0.13	1.87	−0.40
$Ag_{17}Cu_{23}$	c-Dh	C_s	0	0.13	1.88	−0.25
$Ag_{20}Cu_{20}$	c-pc5	C_s	0	0.77	0.00	0.00
$Ag_{20}Cu_{20}$	c-pc6	D_{6h}	0	0.09	2.38	−0.09
$Ag_{22}Cu_{18}$	c-pc5	C_{5v}	0	0.78	0.00	0.00
$Ag_{26}Cu_{14}$	c-pc5	C_s	0	0.77	0.00	0.00
$Ag_{27}Cu_{13}$	c-pc5	C_{5v}	0	0.80	0.00	0.00
$Ag_{28}Cu_{12}$	c-pc5	C_s	0	0.77	0.00	0.00
$Ag_{32}Cu_8$	c-pc5	C_{5v}	0	0.75	0.00	0.00
$Ag_{32}Cu_8$	c-pc6	D_{6h}	0	0.06 JT[e]	1.61	0.09
$Ag_{33}Cu_7$	c-pc5	C_{5v}	0	0.71	0.00	0.00
$Ag_{34}Cu_6$	c-pc5	C_s	0	0.75	0.00	0.00
$Ag_{34}Cu_6$	c-pc6	C_s	0	0.03	0.73	−0.56
$Ag_{34}Cu_6$	TO[d]	D_{4h}	1	0.54/0.11	2.03	1.34

[a]Capped decahedra. [b] Capped 5-fold pancakes. [c]Capped 6-fold pancakes. [d]fcc-truncated octahedra. [e] JT indicates Jahn−Teller systems. [f]ΔE_{SMTB} is the energy difference within the SMTB model potential (here the zero of the energy is the lowest isomer after DFT optimization). Within the SMTB model, the $Ag_{34}Cu_6$ TO turns out to be highly distorted.

Let us now compare the energetic stability of clusters of different compositions. To this end, we define the excess energy E^*_{exc} as follows

$$E^*_{exc}(Ag_nCu_{N-n}) = E(Ag_nCu_{N-n}) - n\frac{E(Ag_N)}{N} - (N-n)\frac{E(Cu_N)}{N} \quad (1)$$

where $E(Ag_nCu_{N-n})$ is the energy of Ag_nCu_{N-n}, whereas $E(Ag_N)$ and $E(Cu_N)$ are the energies of the homogeneous Ag_{40} and Cu_{40} clusters, respectively. Energy values are obtained by the DFT calculations. For each composition, the lowest-energy isomers are considered. E^*_{exc} is analogous to the formation energy of bulk alloys, adapted to the case of nanoclusters. This quantity is a good indicator of the cluster stability and of the tendency to mixing. As shown in Figure 3, the plot of E^*_{exc} singles out an especially stable composition, corresponding to $n = 27$, where a quite sharp minimum is found. $Ag_{27}Cu_{13}$ is a perfect core−shell cluster, with a central icosahedral Cu core, and an external Ag shell. This is the cluster with the largest inner Cu core, and its special stability is due to the concurrent factors mentioned at the beginning of this section. The special stability of $Ag_{27}Cu_{13}$ is analogous to that of $Ag_{27}Cu_7$ for clusters of size 34.[17]

We can thus hypothesize a natural pathway for the growth of AgCu nanoclusters passing through a series of polyicosahedral clusters of the same family, from pc5 clusters at size 34 (with preferred composition $Ag_{27}Cu_7$) to c-pc5 structures at size 40 (preferred composition $Ag_{27}Cu_{13}$) to the anti-Mackay icosahedron at size 45, of which the previous clusters are fragments.[18]

Finally, to quantify the energy gain due to the electronic shell closure, we have analyzed a series of isomers of $Ag_{27}Cu_{13}$. These isomers (see Figure 4) all belong to the c-pc5 motif. The lowest in energy is the perfect C_{5v} c-pc5 cluster, whereas the other

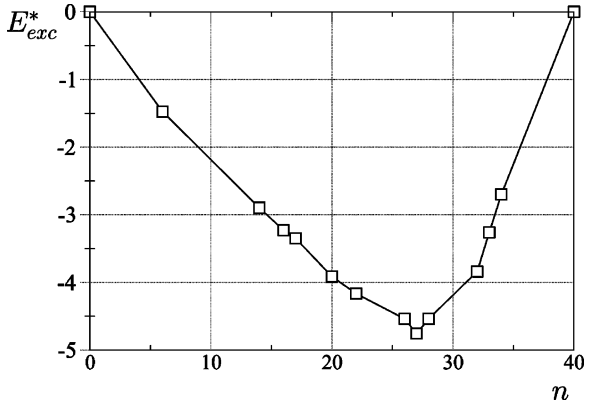

Figure 3. Excess energy E^*_{exc} (see eq 1) as a function of the number of Ag atoms n. Energies are given in eV.

seven isomers are different defected c-pc5 structures. According to the SMTB model, all these isomers are very close in energy, with a maximum ΔE of about 0.06 eV. At variance, at the DFT level, the eight isomers separate into two groups of four. In the first group, all isomers present electronic shell closure, with large gaps between 0.65 and 0.80 eV, and quasi-degenerate total energies (ΔE within 0.05 eV). In the second group, the clusters present small gaps (from 0.21 down to 0.13 eV) and correspondingly considerably higher total energies (ΔE from 0.62 to 1.27 eV). We can thus quantify in ≈0.7 eV the additional stabilization due to electronic shell closure.

6. Polyicosahedral Motifs in AuCu

In the following, we consider c-pc5 and c-pc6 motifs in AuCu 40-atom clusters, showing that the relative stability of the different structures is ruled by rather subtle effects. The qualitative considerations which single out $N = 40$ as a magic electronic size apply also in this case. Moreover, the difference in atomic radii is practically the same for AuCu and AgCu. However, there are two differences which play a key role in determining a different relative structural stability. First of all, compared to AgCu, AuCu has a considerably stronger tendency to form heterogeneous bonds (note that Ag and Cu have an extended miscibility gap in bulk crystals, whereas Au and Cu form a series of ordered alloys). The larger extent of the gold d orbitals (the d orbitals expand with respect to silver due to the relativistic contraction of the gold s orbitals) favors their participation to chemical bonding with copper d orbitals, thus producing a more defined directional character of the Au−Cu interaction with respect to the "isotropic" Ag−Cu interaction. Second, Ag atoms better accommodate bond elongation as compared to Au atoms,[4] due to the shorter-range character of the atom−atom interaction in gold with respect to silver, again ultimately relying on the limited spatial extension (relativistic contraction) of the Au s orbitals. Structures of c-pc5 type are more strained than c-pc6 structures; the latter present also a higher number of heterogeneous bonds at a given composition. These two factors are in favor of c-pc6 structures in the case of AuCu, whereas electronic shell closure is in favor of c-pc5 clusters but with somewhat reduced gaps (see Table 3). Depending on composition, either the geometric and chemical ordering effects or the shell closure effect may prevail, so that, at variance with AgCu, there is a close competition of the two motifs in AuCu clusters. As shown in Table 3, for $Au_{17}Cu_{23}$, the c-pc5 cluster is still lower in energy, but the energy separation ΔE is small. Analogously, for $Au_{28}Cu_{12}$, ΔE is less than 1 eV, which should be compared with the much larger ΔE in AgCu clusters in this composition range. Finally, for $Au_{34}Cu_6$, the stability is reversed, so that the c-pc6 cluster is lower than the c-pc5 by more than 1.5 eV.

TABLE 3: Structure, Symmetry Group, Spin, HOMO−LUMO Gap, and Separation from the Lowest Minimum ΔE for AuCu-Capped 5-Fold Pancakes (c-pc5) and Capped 6-Fold Pancakes (c-pc6)

composition	structure	group	spin	gap (eV)	ΔE (eV)
$Au_{17}Cu_{23}$	c-pc5	C_{5v}	0	0.53	0.00
$Au_{17}Cu_{23}$	c-pc6	D_{3h}	0	0.33	0.18
$Au_{22}Cu_{18}$	c-pc5	C_{5v}	0	0.52	0.00
$Au_{27}Cu_{13}$	c-pc5	C_{5v}	0	0.56	0.00
$Au_{28}Cu_{12}$	c-pc5	C_s	0	0.55	0.00
$Au_{28}Cu_{12}$	c-pc6	C_s	0	0.38	0.81
$Au_{34}Cu_6$	c-pc6	C_s	0	0.25	0.00
$Au_{34}Cu_6$	c-pc5	C_s	0	0.65	1.55

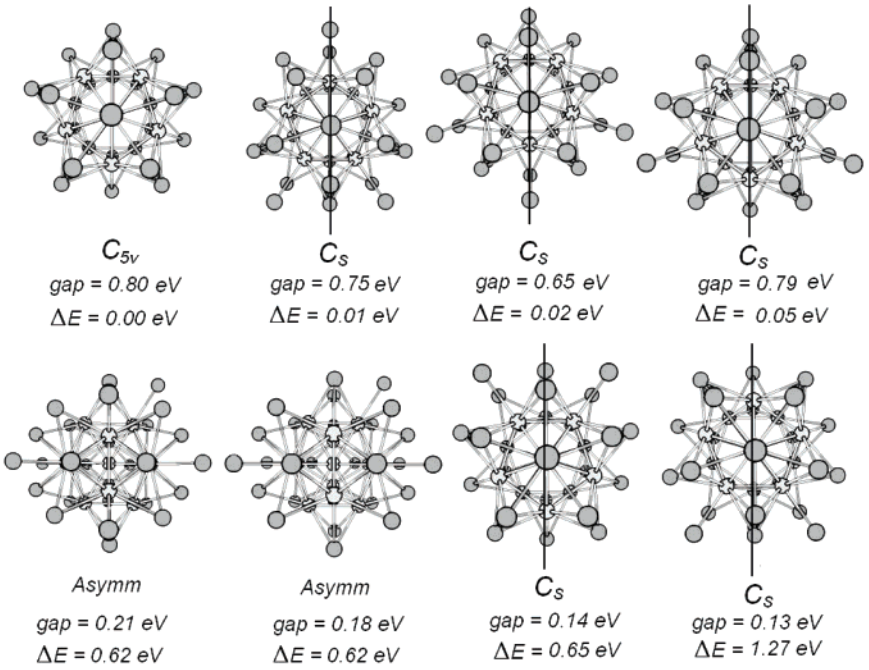

Figure 4. Isomers of $Ag_{27}Cu_{13}$, with HOMO−LUMO gaps and energy separation ΔE.

7. Conclusions

A combined empirical-potential/first-principles analysis of AgCu and AuCu clusters of 40 atoms has shown that the most stable structures originate from a nontrivial interplay of geometric and electronic effects.

Geometric effects include the selection of the structural motif and of the type of chemical ordering. In AgCu, chemical ordering is core−shell, since the larger surface energy of silver with respect to copper produces a tendency to surface segregation of Ag. This tendency is reinforced in polyicosahedral structures, since the relief of internal tension in these structures is favored when inner atoms are of small size compared to surface atoms.[17] These considerations are especially valid when the proportion of silver atoms is not too small. On the Cu-rich side, also, capped decahedral structures can give an efficient geometry optimization.

Moreover, the stability of a structure can be modulated by purely electronic effects. Indeed, the structural motif presenting an electronic shell closure becomes by far the dominant one in AgCu. This motif is the capped 5-fold pancake: thus c-pc5 clusters combine an optimal geometric structure with an optimal electronic structure. Conversely, an electronic shell unclosure effect destabilizes the c-pc6 and fcc-truncated octahedral structures. The high stability of c-pc5 structures suggests a natural growth pathways through polyicosahedral clusters leading to the anti-Mackay icosahedron of 45 atoms.

The fact that geometric and quantum effects concur to favor magic structures associated with core−shell chemical ordering and high symmetry renders these clusters very promising from the point of view of their optical properties (investigation along these lines is in progress in our labs).

In other cases one can find a delicate balance between geometric and electronic factors. In AuCu, in fact, c-pc5 structures are less optimal from the geometric point of view (both because of too strained bonds and of chemical ordering with too little intermixing), so that the gain due to electronic shell closure may not be sufficient for some compositions to compensate for these factors. Therefore, in AuCu, c-pc5 and c-pc6 structures are in close competition.

Acknowledgment. We acknowledge financial support from the Italian CNR for the project "(Supra)-Self-Assemblies of Transition Metal Nanoclusters" within the framework of the ESF EUROCORES SONS and from European Community Sixth Framework Program for the project "Growth and Supra-Organization of Transition and Noble Metal Nanoclusters" (Contract No. NMP4-CT-2004-001594).

References and Notes

(1) De Heer, W. A. *Rev. Mod. Phys.* **1993**, *65*, 611.
(2) Alonso, J. A. *Chem. Rev.* **2000**, *100*, 637.
(3) Heiz, W.; Schneider, W. D. *J. Phys. D: Appl. Phys.* **2000**, *33*, R85.
(4) Baletto, F.; Ferrando, R. *Rev. Mod. Phys.* **2005**, *77*, 371.
(5) Pyykkö, P. *Angew. Chem., Int. Ed.* **2004**, *43*, 4412.
(6) Schooss, D.; Blom, M. N.; Parks, J. H.; von Issendorf, B.,; Haberland, H.; Kappes, M. M. *Nano Lett.* **2005**, *5*, 1972.
(7) Xing, X.; Danell, R. M.; Garzón I. L.; Michaelian, K.; Blom, M. N.; Burns, M. M.; Parks, J. H. *Phys. Rev. B: Condens. Matter Mater. Phys.* **2005**, *72*, 081405.
(8) Knickelbein, M. B.; Koretsky, G. M. *J. Phys. Chem. A* **1998**, *102*, 580.
(9) Kim, Y. D. *Int. J. Mass Spectrom.* **2004**, *238*, 17.
(10) Bernhardt, T. M. *Int. J. Mass Spectrom.* **2005**, *243*, 1.
(11) Schmidt, M.; Masson, A.; Bréchignac C. *J. Chem. Phys.* **2005**, *122*, 134712.
(12) Ichihashi, M.; Corbett, C. A.; Hanmura, T.; Lisy, J. M.; Kondow, T. *J. Phys. Chem. A* **2005**, *109*, 7872.
(13) Nepijiko, S. A.; Ievlev, D. N.; Schulze, W. *Eur. Phys. J. D* **2003**, *24*, 115.
(14) Celep, G.; Cottancin, E.; Lermé, J.; Pellarin, M.; Arnaud, L.; Huntzinger, J. R.; Vialle, J. L.; Broyer, M.; Palpant, B.; Boisron, O.; Mélinon, P. *Phys. Rev. B*: *Condens. Matter Mater. Phys.* **2004**, *70*, 165409.
(15) Padeletti, G.; Fermo, P. *Appl. Phys. A: Mater. Sci. Process.* **2003**, *76*, 515.
(16) Darby, S.; Mortimer-Jones, T. V.; Johnston, R. L.; Roberts, C. *J. Chem. Phys.* **2002**, *116*, 1536.
(17) Rossi, G.; Rapallo, A.; Mottet, C.; Fortunelli, A.; Baletto, F.; Ferrando, R. *Phys. Rev. Lett.* **2004**, *93*, 105503.
(18) Ferrando, R.; Fortunelli, A.; Rossi, G. *Phys. Rev. B: Condens. Matter Mater. Phys.* **2005**, *72*, 085449.
(19) Rapallo, A.; Rossi, G.; Ferrando, R.; Fortunelli, A.; Curley, B. C.; Lloyd, L. D.; Tarbuck, G. M.; Johnston, R. L. *J. Chem. Phys.* **2005**, *122*, 194308.
(20) Pauwels, B.; Van Tendeloo, G.; Zhurkin, E.; Hou, M.; Verschoren, G.; Theil Kuhn, L.; Bouwen, W.; Lievens, P. *Phys. Rev. B: Condens. Matter Mater. Phys.* **2001**, *63*, 165406.
(21) Janssens, E.; Neukermans, S.; Wang, X.; Veldeman, N.; Silverans, R. E.; Lievens, P. *Eur. Phys. J. D* **2004**, *34*, 23.
(22) Cazayous, M.; Langlois, C.; Oikawa, T.; Ricolleau, C.; Sacuto, A. *Phys. Rev. B: Condens. Matter Mater. Phys.* **2006**, *73*, 113402.
(23) Kumar, V. *Comput. Mater. Sci.* **2006**, *36*, 1.
(24) Massen, C.; Mortimer-Jones, T. V.; Johnston, R. L. *J. Chem. Soc., Dalton Trans.* **2002**, 4375.
(25) Baletto, F.; Mottet, C.; Ferrando, R. *Phys. Rev. Lett.* **2003**, *90*, 135504.
(26) Fromen, M. C.; Morillo, J.; Casanove, M. J.; Lecante, P. *Europhys. Lett.* **2006**, *73*, 885.
(27) Katakuse, I.; Ichihara, T.; Fujita, Y.; Matsuo, T.; Sakurai, T.; Matsuda, H. *Int. J. Mass. Spectrom. Ion Proc.* **1985**, *67*, 229.
(28) Taylor, K. J.; Pettiette-Hall, C. L.; Cheshnovsky, O.; Smalley, R. E. *J. Chem. Phys.* **1992**, *96*, 3319.
(29) Jackschath, C.; Rabin, I.; Schulze, W. Z. *Phys. D*: *Amsterdam, Neth.* **1992**, *22*, 517.
(30) Alameddin, G.; Hunter, J.; Cameron, D.; Kappes, M. M. *Chem. Phys. Lett.* **1992**, *192*, 122.
(31) Cha, C.-Y.; Ganteför, G.; Eberhardt, W. J. *J. Chem. Phys.* **1993**, *99*, 6308.
(32) Handschuh, H.; Bechthold, P. S.; Ganteför, G.; Eberhardt, W. J. *J. Chem. Phys.* **1994**, *100*, 7093.
(33) Brack, M. *Rev. Mod. Phys.* **1993**, *65*, 677.
(34) Stone, A. J. *Inorg. Chem.* **1981**, *20*, 563.
(35) Wales, D. J.; Stone, A. J. *Inorg. Chem.* **1989**, *28*, 3120.
(36) Johnston, R. L.; Mingos, D. M. P. *J. Chem. Soc., Dalton Trans.* **1987**, 1445.
(37) Hirsch, A.; Chen, Z.; Jiao, H. *Angew. Chem., Int. Ed.* **2000**, *39*, 3915.
(38) Tsipis, C. A. *Coord. Chem. Rev.* **2005**, *249*, 2740.
(39) Rossi, G.; Ferrando, R.; Rapallo, A., Fortunelli, A.; Curley, B. C.; Lloyd, L. D.; Johnston, R. L. *J. Chem. Phys.* **2005**, *122*, 194309.
(40) Aprà, E.; Ferrando, R.; Fortunelli, A. *Phys. Rev. B*: *Condens. Matter Mater. Phys.* **2006**, *73*, 205414.
(41) Jellinek, J.; Krissinel, E. B. *Chem. Phys. Lett.* **1996**, *258*, 283.
(42) Gupta, R. P. *Phys. Rev. B*: *Solid State* **1981**, *23*, 6265.
(43) Cleri, F.; Rosato, V. *Phys. Rev. B: Condens. Matter Mater. Phys.* **1993**, *48*, 22.
(44) Baletto, F.; Mottet, C.; Ferrando R. *Phys. Rev. B: Condens. Matter Mater. Phys.* **2002**, *66*, 155420.
(45) Meunier, I.; Tréglia, G.; Gay, J. M.; Aufray, B.; Legrand, B. *Phys. Rev. B: Condens. Matter Mater. Phys.* **1999**, *50*, 10910.
(46) Doye, J. P. K.; Wales, D. J. *J. Phys. Chem. A* **1997**, *101*, 5111.
(47) Hansmann, U. H. E.; Wille, L. T. *Phys. Rev. Lett.* **2002**, *88*, 068105.
(48) Rossi, G.; Ferrando, R. *Chem. Phys. Lett.* **2006**, *423*, 17.
(49) ELP and PEW are especially suited for exploring potential energy surfaces exhibiting structurally different basins of attraction and require the use of an order parameter. As order parameter we have chosen the number of heterogeneous AgCu nearest-neighbor bonds to differentiate the various structural families.
(50) Aprà, E. et al. *NWChem, A Computational Chemistry Package for Parallel Computers*, Version 4.7; Pacific Northwest National Laboratory: Richland, WA, USA, 2005.
(51) Becke, A. D. *Phys. Rev. A* **1988**, *38*, 3098.
(52) Perdew, J. P.; Chevary, J. A.; Vosko, S. H.; Jackson, K. A.; Pederson, M. R.; Singh, D. J.; C. Fiolhais, C. *Phys. Rev. B* **1992**, *46*, 6671.
(53) Schaefer, A.; Huber, C.; Ahlrichs, R. *J. Chem. Phys.* **1994**, *100*, 5289.
(54) Andrae, D.; Haeussermann, U.; Dolg, M.; Stoll, H.; Preuss, H. *Theor. Chim. Acta* **1990**, *77*, 123.
(55) Dolg, M.; Wedig, U.; Stoll, H.; Preuss, H. *J. Chem. Phys.* **1987**, *86*, 866.
(56) ftp://ftp.chemie.uni-karlsruhe.de/pub/basen.

(57) Aprà, E.; Fortunelli, A. *J. Phys. Chem.* **2003**, *107*, 2934.
(58) Courtesy of Dr. Florian Weigend, Karlsruhe, Germany.
(59) (a) Elsässer, C.; Fähnle, M.; Chan, C. T.; Ho, K. M. *Phys. Rev. B: Condens. Matter Mater. Phys.* **1994**, *49*, 13975. (b) Warren, R. W.; Dunlap, B. I. *Chem. Phys. Lett.* **1996**, *262*, 384.
(60) Doye, J. P. K.; Wales, D. J. *New J. Chem.* **1998**, *22*, 733.
(61) Doye, J. P. K. *J. Chem. Phys*. **2003**, *119*, 1136.
(62) We chose $A = 10.9$ eV and $r_0 = 5.6$ Å, such that the Extended Hückel DOS around the Fermi level optimally matches the DFT DOS.
(63) Doye, J. P. K.; Meyer, L. *Phys. Rev. Lett.* **2005**, *95*, 063401.
(64) Pauling, L. *The Nature of the Chemical Bond*; Cornell University Press: Ithaca, NY, 1960.